Utilizing a shallow trench isolation parasitic transistor to characterize the total ionizing dose effect of partially-depleted silicon-on-insulator input/output n-MOSFETs*

Peng Chao(彭 超)[a], Hu Zhi-Yuan(胡志远)[a], Ning Bing-Xu(宁冰旭)[a], Huang Hui-Xiang(黄辉祥)[a], Fan Shuang(樊 双)[a], Zhang Zheng-Xuan(张正选)[a]†, Bi Da-Wei(毕大炜)[a], and En Yun-Fei(恩云飞)[b]

[a] *State Key Laboratory of Functional Materials for Informatics, Shanghai Institute of Microsystem and Information Technology, Chinese Academy of Sciences, Shanghai* 200050, *China*

[b] *Science and Technology on Reliability Physics and Application Technology of Electronic Component Laboratory, Guangzhou* 510610, *China*

(Received 11 March 2014; revised manuscript received 25 March 2014; published online 16 July 2014)

We investigate the effects of ^{60}Co γ-ray irradiation on the 130 nm partially-depleted silicon-on-isolator (PDSOI) input/output (I/O) n-MOSFETs. A shallow trench isolation (STI) parasitic transistor is responsible for the observed hump in the back-gate transfer characteristic curve. The STI parasitic transistor, in which the trench oxide acts as the gate oxide, is sensitive to the radiation, and it introduces a new way to characterize the total ionizing dose (TID) responses in the STI oxide. A radiation enhanced drain induced barrier lower (DIBL) effect is observed in the STI parasitic transistor. It is manifested as the drain bias dependence of the radiation-induced off-state leakage and the increase of the DIBL parameter in the STI parasitic transistor after irradiation. Increasing the doping concentration in the whole body region or just near the STI sidewall can increase the threshold voltage of the STI parasitic transistor, and further reduce the radiation-induced off-state leakage. Moreover, we find that the radiation-induced trapped charge in the buried oxide leads to an obvious front-gate threshold voltage shift through the coupling effect. The high doping concentration in the body can effectively suppress the radiation-induced coupling effect.

Keywords: partially depleted silicon-on-isolator n-MOSFET, sidewall implant, shallow trench isolation, total ionizing dose

PACS: 07.89.+b, 42.88.+h, 85.30.–z **DOI:** 10.1088/1674-1056/23/9/090702

1. Introduction

The natural space radiation environment consists of different kinds of extremely energetic particles, including energetic protons, electrons, and heavy ions.[1,2] The integrated circuits (ICs) used in a space system must endure all of these space environmental hazards and meet their performance requirements. One of the most important radiation effects affecting the reliability of the ICs is the total ionizing dose (TID) effect. It is a long-term radiation effect which includes the effects related to the interaction of the energetic particles with the insulator in the metal–oxide–semiconductor field-effect transistors (MOSFET).[3,4] The energetic particles deposit energy and generate trapped charge in the insulator. Finally, the trapped charge located in the insulator or at the interface leads to the degradation of the characteristics of the MOSFET.[5] The effects of ionizing radiation on discrete n- and p-channel MOS transistors are correlated with the performance degradation of CMOS integrated circuits. To make the ICs operate stably, safely, and reliably in the space radiation environment, the discrete MOSFETs must be carefully designed.

Silicon-on-insulator (SOI) MOSFETs have several intrinsic potential advantages over their bulk Si counterparts for the operation in radiation-harsh environments.[6] In particular, the thin semiconductor film and the buried oxide (BOX) layer provide better resistance against the transient ionization effects, like single event upsets or latch-up.[7,8] However, the thick BOX introduces an additional constraint due to total ionizing dose charge trapping and makes the TID effect become more complex. The radiation-induced trapped charge in the BOX causes the increase of the leakage current in the subthreshold region for partially-depleted (PD) SOI n-MOSFETs and the decrease of the front-gate threshold voltage for fully-depleted (FD) SOI n-MOSFETs.[9] The previous literature shows that the amount of radiation-induced defect buildup in an oxide is proportional to the oxide thickness.[10] For a gate oxide less than 7 nm thick, the defect buildup in the gate dielectric is often negligible. The continuous miniaturization process has implicitly led to radiation-hard front gate oxides, with a thickness below the trapped-hole tunneling limit.[11] However, the shallow trench isolation (STI) oxide used to isolate the transistors does not scale down and still has a large thickness, therefore this oxide is expected to be very sensitive to radiation.[12–14]

To ensure the radiation hardness of devices in space systems, laboratory radiation tests must be performed. In this

*Project supported by the Opening Project of Science and Technology on Reliability Physics and Application Technology of Electronic Component Laboratory, China (Grant No. ZHD201205) and the National Natural Science Foundation of China (Grant No. 61106103).

†Corresponding author. E-mail: zxzhang@mail.sim.ac.cn

© 2014 Chinese Physical Society and IOP Publishing Ltd

paper, the TID effects of a 130 nm short channel PDSOI input/output (I/O) n-MOSFET are investigated using a laboratory radiation source. The high voltage I/O transistor is one commonly used MOS device in modern CMOS ICs. It usually has a thicker gate oxide, a higher threshold voltage, and a low body doping compared to the core devices, and is traditionally available to allow the integration of low power ICs within systems requiring higher logic levels. We propose an STI parasitic transistor model to explain the hump effect in the back-gate transfer characteristic curve. The STI parasitic transistor is sensitive to the radiation, and the variation of the characteristic of the STI parasitic transistor after radiation can be used to characterize the TID responses of the PDSOI n-MOSFET. The drain bias during measurement, the body doping concentration, and the STI sidewall implantation are found to have strong influences on the electrical parameter of the STI parasitic transistor (e.g., threshold voltage), thus further affect the TID effect of the device. These are the design issues that should be optimized to develop a radiation-hardened technology.

2. Experimental details

All the devices used in our experiment were fabricated in 130 nm PDSOI technology. A 200 mm diameter UNIBOND^{TM} wafer from SOITEC was used. The top Si film and the buried oxide were approximately 100 nm ($\pm$10 nm) and 145 nm ($\pm$6 nm) thick, respectively. The resistivity of the top silicon layer was 8.5–11.5 Ω·cm. All the samples used in the experiment were I/O devices with a gate oxide thickness of 6.8 nm and $W/L = 10$ μm/0.35 μm. Due to the sacrificial oxidation and the gate oxide growth, the final top silicon thickness was 80 nm. All the devices had a 130 nm thick polysilicon gate and a 65 nm wide L-shaped spacer. A T-shape gate was introduced as the body contact. The STI which connected with the buried oxide at the bottom was introduced for isolation. No halo doping was applied in the I/O device. For PDSOI n-MOSFETs, a parasitic n–p–n bipolar transistor was formed in the neutral region of the thin film. The emitter and the collector of the parasitic bipolar transistor were the the source and the drain of the n-MOSFET, respectively. All the samples were 24-pin DIP ceramic packaged. The operating voltage was 3.3 V.

The experiments were conducted in Xinjiang Technical Institute of Physics and Chemistry, the Chinese Academy of Sciences, and ^{60}Co γ-ray was used as the radiation source. The dose rate was typically around 100 rad(Si)/s. During the radiation exposure, the devices were under ON bias with the gate biased at 3.3 V and the other terminals grounded. This has been proved to be the worst bias condition during the total dose irradiation for our devices. Before irradiation and after every irradiation step, the I–V characteristics of the devices were measured by a Keithley 4200B parameter analyzer at room temperature. The I–V measurements were taken for both the front-gate and the back-gate transistors. The back-gate transistor consisted of the substrate (gate), the BOX (gate insulator), the source, the drain, and the body of the front-gate transistor. All the I–V curves were taken within half an hour following exposure.

3. Results and discussion

3.1. STI parasitic transistor

Figure 1 shows the back gate transfer characteristics of a 10/0.35 PDSOI n-MOSFET with drain bias at 0.1 V before and after irradiation. A hump is observed at the subthreshold region both in the pre- and the post-irradiation I–V curves. The back-gate hump is assumed to correlate with the STI parasitic transistor near the STI bottom corner. This parasitic transistor, in which the substrate of the main transistor acts as the gate electrode and the trench oxide serves as the gate oxide, gives rise to an additional leakage path along the vertical trench sidewall. The measured transfer characteristic curve of the back-gate transistor is actually the superposition of the transfer characteristic of the STI parasitic transistor and that of the back-gate main transistor. The characteristic of the parasitic transistor is sensitive to the shape of the trench bottom corner.[15] In the trench-etch process, over-etching of the silicon to expose the buried oxide along with no proper bottom corner rounding can lead to an abrupt transition from the buried oxide to the trench oxide. Thus, the effective oxide thickness is usually small in the bottom corner region. The thin oxide can enhance the electric field in this region and reduce the threshold voltage of the bottom corner parasitic transistor. The threshold voltage of the STI parasitic transistor ($V_{t,STI}$) becomes less than that of the back-gate main transistor ($V_{t,bg}$), so an obvious hump can be observed. Even though the back-gate hump enhances the total ionizing dose susceptibility in the PDSOI n-MOSFET, the variation of the hump, i.e., the transfer characteristic of the STI parasitic transistor, after irradiation introduces a new way to characterize the total ionizing dose responses.

The effective threshold voltage of the STI parasitic transistor ($V_{t,STI}$) can be expressed as[16]

$$V_{t,STI} = \psi_{ms} + 2\psi_F - \frac{Q_{STI}}{C_{STI}} + \frac{\sqrt{4q\varepsilon_{Si}N_A\psi_F}}{C_{STI}}, \quad (1)$$

$$\psi_F = \frac{KT}{q}\ln\left(\frac{N_A}{n_i}\right), \quad (2)$$

where ε_{Si} is the permittivity of silicon, n_i is the intrinsic carrier concentration, ψ_{ms} is the work function difference between the gate of the parasitic device and the p-type body, ψ_F is the Fermi potential, Q_{STI} is the effective charge density in the STI oxide, C_{STI} is the effective gate capacitance per unit area

of the parasitic device, and N_A is the body doping concentration. After irradiation, the radiation-induced positive charge is trapped both in the buried oxide and the STI oxide, which are the gate oxide of the back-gate main transistor and that of the STI parasitic transistor, respectively. A large amount of positive charge deposits in the STI oxide and increases Q_{STI}. The additional Q_{STI} leads to the reduction of the threshold voltage of the STI parasitic transistor and causes a large negative shift of the hump ($\Delta V_{t,STI}$), so is the back-gate main transistor ($\Delta V_{t,bg}$), as shown in Fig. 1.

The effective threshold voltage of the STI parasitic transistor after different total dose radiations can be extracted. The threshold voltage is defined as the gate voltage at which I_{ds} reaches $(W_{STI}/L_{STI})\times 10^7$ A for the STI parasitic transistor, where W_{STI} and L_{STI} are the effective channel width and length of the STI parasitic device, respectively. For simplicity, we assume W_{STI} equal to the top silicon film thickness and L_{STI} equal to the channel length of the main transistor. That is to say, $W_{STI} = 80$ nm and $L_{STI} = 0.35$ μm. For the device in Fig. 1, the threshold voltage of the STI parasitic device before irradiation is 4.55 V. After 500 krad(Si) irradiation, the threshold voltage of the STI parasitic device is lower than 0 V ($V_{t,STI} = -5.85$ V). This means that the device cannot be cut off when $V_{fg} = V_{bg} = 0$ V due to the turning on of the parasitic transistor. The STI parasitic transistor leads to a large off-state leakage current (nearly 10^{-6} A after 500 krad(Si) radiation) which can hardly be modulated by the front-gate voltage. Although a large negative shift (7.7 V) is also observed, the back-gate threshold voltage is 4.6 V at 500 krad(Si). That is, a certain margin still exists for the back-gate transistor. The radiation-induced trapped charge in the STI oxide, but not in the buried oxide, becomes the leading cause of the intra device leakage after ON bias irradiation.

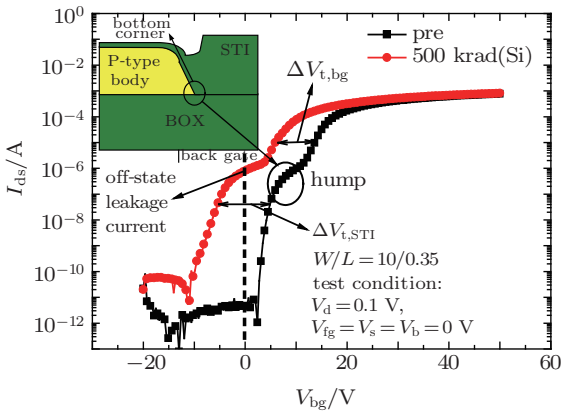


Fig. 1. (color online) Back-gate transfer characteristic curves of a 10/0.35 PDSOI I/O n-MOSFET with drain biased at 0.1 V before and after irradiation. An STI parasitic transistor located near the bottom corner is added to the back-gate main transistor. The STI parasitic transistor consists of substrate (gate), STI oxide (gate oxide), source/drain/body of the main transistor.

3.2. Impact of the drain bias during measurement

Figure 2 shows the off-state leakage current as a function of the total ionizing dose for a 10/0.35 PDSOI I/O n-MOSFET with different drain biases. The off-state leakage current is extracted with the front gate and the back gate grounded. The radiation-induced off-state leakage in the short channel device not only increases with increasing total dose, but also increases sharply with increasing drain bias voltage. The off-state leakage current at $V_{ds} = 3.3$ V is more than two orders of magnitude higher than the corresponding value at $V_{ds} = 0.1$ V after 100 krad(Si) radiation.

Figure 3 shows the back-gate transfer characteristic curves of a 10/0.35 PDSOI n-MOSFET with the drain biased at 0.1 V and 3.3 V before and after irradiation. Before irradiation, $V_{t,STI} = 5.3$ V at $V_d = 0.1$ V and $V_{t,STI} = 4.4$ V at $V_d = 3.3$ V. The lower threshold voltage at the high drain voltage indicates the drain induced barrier lower (DIBL) effect in the STI parasitic transistor. As discussed above, the STI parasitic transistor is the main contributor to the radiation-induced off-state leakage current. The smaller threshold voltage implies less margin existing under the high drain bias. This can explain the observed larger leakage current at a higher drain voltage. Moreover, the radiation-induced charge in the trench oxide raises the nearby body potential and further lowers the source-to-body potential barrier when the channel length is short enough.[17] Then the observed DIBL effect in the STI parasitic is enhanced by the radiation, and it is manifested with the increase of the DIBL parameter after radiation. The DIBL parameter, which is defined as the change in the threshold voltage divided by the change in the drain voltage, is 0.30 and 0.73 before and after 50 krad(Si) radiation. The greater DIBL parameter in the STI parasitic transistor means a further reduction in the threshold voltage at a high drain voltage. This also results in the increase of the leakage current with increasing drain bias. In practice, the radiation response of a submicron device should be paid more attention for the drain bias dependence, especially for the short channel device.

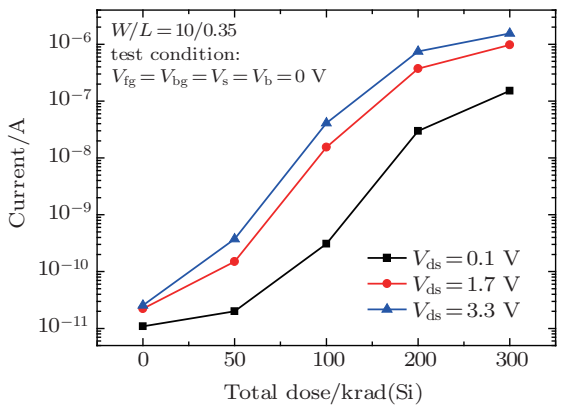


Fig. 2. (color online) Off-state leakage current as a function of the total ionizing dose for a 10/0.35 PDSOI I/O n-MOSFET with different drain biases. The off-state leakage current is extracted with the front gate and the back gate grounded, i.e., $V_{fg} = V_{bg} = 0$ V.

It is interesting to notice the abrupt transition from the subthreshold region to the saturation region when the drain bias is 3.3 V, as shown in Fig. 3. It reveals the influence of the parasitic bipolar transistor in the neutral body region. When the drain bias is large enough in the short channel device, electrons in the channel of the n-MOSFET acquire more than 1.5 eV energy, the impact ionization can occur.[18] The holes generated during the process of the impact ionization accumulate in the body and can significantly modulate the potential at the source/body junction due to the small spacing between the source and the drain in the short channel device. This can forward bias the body–source junction, trigger the parasitic bipolar conduction, and lead to the abrupt increase in the drain current. As reported for the PD device in the previous paragraph, the existence of the body contact can suppress the parasitic bipolar effect.[19] However, the high body impedance makes the external body contact ineffective in the region far away from the contact point, and the local parasitic bipolar effect still occurs. This effect will degrade the hardness of the SOI circuits.[8,20]

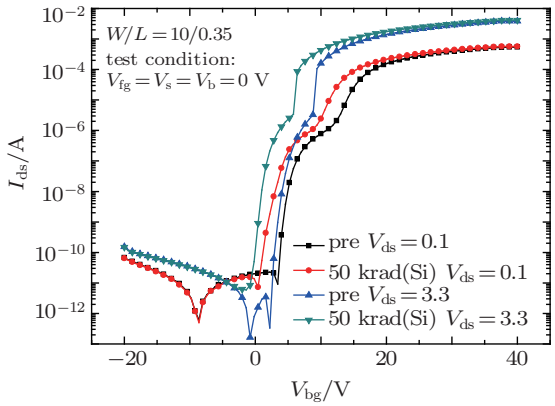


Fig. 3. (color online) Back-gate transfer characteristic curves of a 10/0.35 PDSOI n-MOSFET with the drain biased at 0.1 V and 3.3 V before and after irradiation. The bias condition is $V_{fg} = V_{source} = V_{body} = 0$ V.

3.3. Impact of the body doping concentration

To design a radiation hardened device, a key method is adjusting the threshold voltage of the STI parasitic transistor. The larger the threshold voltage, the more hardened the device. According to Eqs. (1) and (2), the threshold voltage of the STI parasitic transistor is proportional to the body doping concentration N_A. We can expect that a high doping concentration in the body will enhance the device's resistance against the total ionizing dose effect. Figure 4 shows the simulated body doping profiles of two samples with different well-implantation conditions. The simulations are performed using the Sentaurus process tool and the process conditions used in the simulation come from the foundry. The maximum body doping concentration of sample 2 is twice as large as that of sample 1. The back-gate transfer characteristics of the two devices with different body doping concentrations are shown in Fig. 5(a). The higher body doping in sample 2 results in higher threshold voltages for the back-gate main transistor and the STI parasitic transistor. The whole back-gate transfer characteristic curve shifts toward the positive direction with a higher body doping. This makes the device less sensitive to the radiation-induced degradation. Figure 5(b) shows the off-state leakage as a function of the total dose for the two devices with different body dopings. No obvious radiation-induced leakage is observed when the dose is up to 200 krad(Si) for sample 2, whereas the off-state leakage in sample 1 increases significantly with increasing total dose. At 100 krad(Si), the extracted leakage is four orders of magnitude larger than the pre-radiation value.

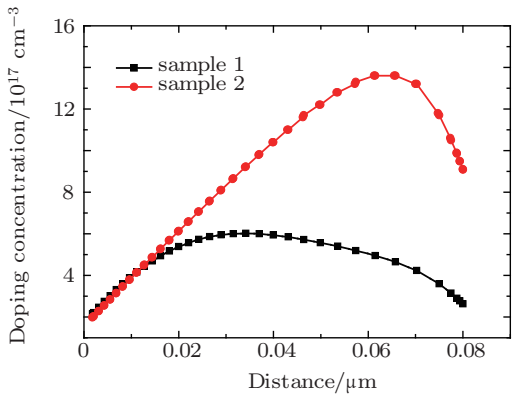


Fig. 4. (color online) Simulated body doping profiles for two devices with different well-implantation conditions. The process conditions used in the simulation come from the foundry.

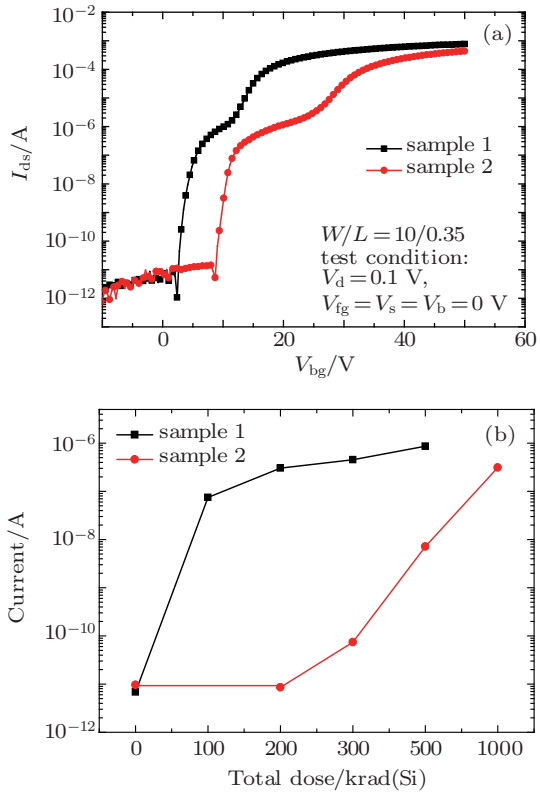


Fig. 5. (color online) (a) Back-gate transfer characteristics of two devices with different body doping concentrations. (b) Off-state leakage current as a function of the total ionizing dose for two devices with different body doping concentrations.

Figure 6 shows the front-gate threshold voltage shift as a function of the total dose for two samples with different body doping concentrations. The observed threshold voltage shift of sample 1 linearly increases with increasing total dose and reaches −138 mV at 500 krad(Si). For sample 2, the observed threshold voltage shift is much smaller than that of sample 1. Up to 500 krad(Si), the threshold voltage is only about −20 mV. The only difference between sample 1 and sample 2 is the doping concentration in the body. So we can conclude that the large discrepancy of the radiation-induced front-gate threshold voltage results from the different body doping. To investigate the mechanism of the radiation-induced threshold voltage shift in the front gate, the simulated depleted regions in the body before and after radiation for samples 1 and 2 are presented in Fig. 7. In the PDSOI devices, the existence of the neutral body separates the contribution of the front gate oxide from that of the buried oxide, and no correlation exists between the front and the back gate transistors.[21] After radiation, the positive charge trapped in the buried oxide will deplete the back surface. If the thickness of the top silicon film (t_{Si}) is less than twice the value of $X_{d,max}$, the depletion zones arising from the front ($X_{d,max}$) and the back interfaces ($X_{d,bg}$) could interconnect together when enough charge is trapped in the buried oxide. At this time, the partially-depleted transistor works like a fully-depleted one. The front and the back gates couple in the PDSOI device, and the front-gate threshold voltage $V_{t,fg}$ shift is then highly influenced by the back-gate threshold voltage $V_{t,bg}$ shift induced by buried oxide trapping. So an obvious negative shift of the front gate threshold voltage can be observed. Since the depletion width is inversely proportional to the body doping, sample 1 with lower body doping has a larger back gate depletion width than sample 2 after the same radiation dose. The width of the depletion region in sample 1 after radiation meets the condition

$$t_{Si} < X_{d,max} + X_{d,bg}. \tag{3}$$

The entire top silicon film is depleted and sample 1 becomes a fully-depleted device (Fig. 7(a)). Thanks to the high body doping concentration, the top silicon thickness (t_{Si}) keeps larger than the sum of the front channel and the back channel depletion region widths ($X_{d,max} + X_{d,bg}$) in sample 2 after the same dose radiation. A neutral body region always exists and sample 2 is still a partially-depleted one (Fig. 7(b)). The radiation-induced large back-gate threshold voltage will couple to the front gate in sample 1, but not in sample 2. This can explain the large differences in the front-gate threshold voltage shift between samples 1 and 2.

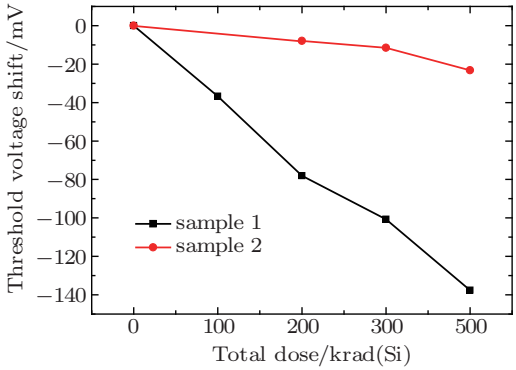


Fig. 6. (color online) Front-gate threshold voltage shift as a function of total ionizing dose for two devices with different body doping concentrations.

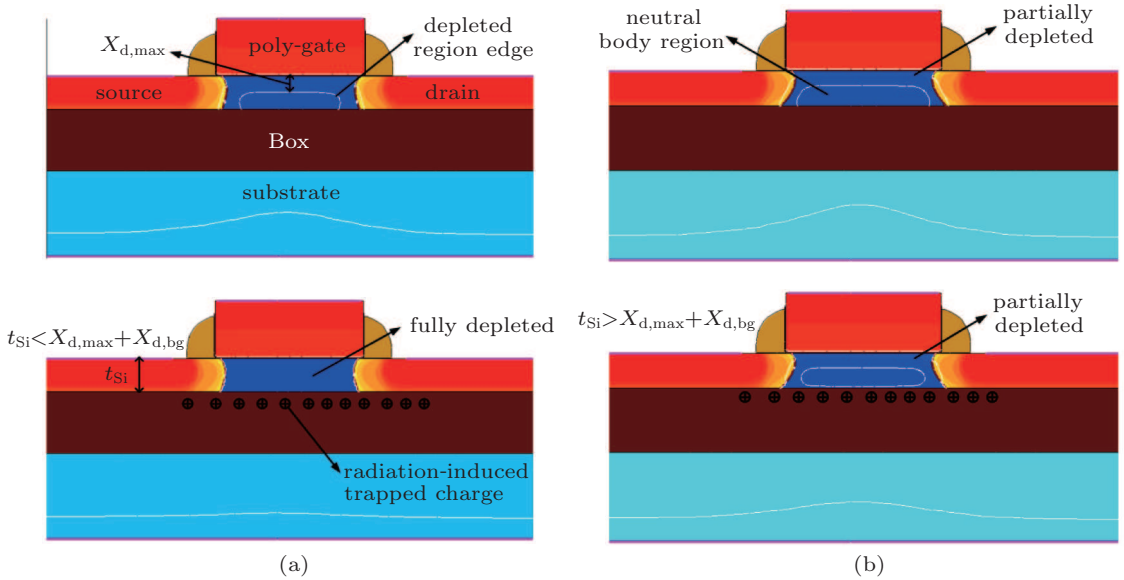


Fig. 7. (color online) Simulated depleted region in the body for PDSOI n-MOSFET before and after irradiation. After radiation, positive charge with density of 1.4×10^{12} cm^{-2} is placed at the BOX/body interface. The bias condition is $V_{fg} = 3.3$ V, $V_d = 0.1$ V, and $V_s = V_{bg} = 0$ V. (a) Sample 1 with low body doping. (b) Sample 2 with high body doping. The body doping concentrations of the two devices are shown in Fig. 4.

3.4. Impact of the STI sidewall implant

Increasing the body doping concentration is an effective way to harden the device and a much lower radiation-induced off-state leakage is observed in the high doping device. However, the characteristics of the main transistor are also changed, since the whole body doping profile is altered. In order to eliminate the influence on the main transistor, a low-title-angle STI sidewall implant is introduced in the STI process.

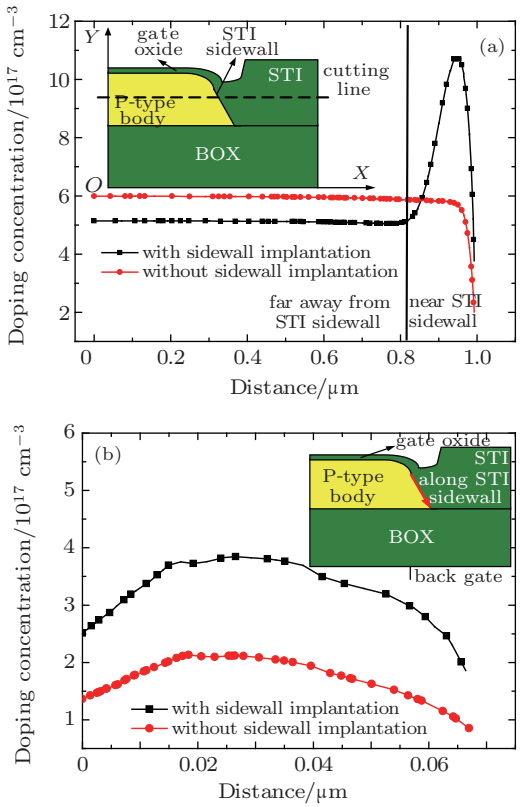


Fig. 8. (color online) Simulation doping concentration in the p-type body as a function of the distance for two samples (one has the sidewall implant, the other one has not): (a) along the channel width direction (cutting line), (b) along STI sidewall. The process conditions used in the simulation come from the foundry.

Figure 8(a) shows the simulated body doping concentration along the channel width direction in the middle of the body (marked by the cutting line) for two samples. One has the sidewall implant, and the other one has not. At the region far away from the sidewall, the body doping concentration is 5.0–6.0×10^{17} cm^{-3}, and it remains constant. The sidewall implant only alters the body doping concentration near the STI sidewall. The peak value of the concentration reaches 1.1×10^{18} cm^{-3} for the sample with the sidewall implant and is nearly twice as large as the sample without the sidewall implant. It is worth noting that the surface concentration at the sidewall/body interface for the sample without the sidewall implant is reduced to 2.0×10^{17} cm^{-3}. The decrease of the doping concentration near the sidewall/body interface may be related to the STI liner oxide process. To minimize the interface charge, a thin, good-quality thermal-oxide layer (STI liner oxide) must be grown inside the trench. During this thermal oxidation, some of the born dopants in the p-type body will segregate into the oxide.[22] After the sidewall implant, the doping concentration along the sidewall/body interface increases significantly, as shown in Fig. 8(b).

The increased body doping concentration near the STI sidewall leads to the increase of the threshold voltage of the STI parasitic transistor, as illustrated in Fig. 9(a). The threshold voltages of the STI parasitic transistors for the samples with and without the sidewall implant are 7.1 V and 4.5 V, respectively. Since the doping concentration near the back channel is not altered by the sidewall implant, the threshold voltages of the back-gate main transistors for the two samples are equal. The data presented in Fig. 9(b) indicate that the device with the sidewall implant exhibits a higher degree of radiation tolerance than that without the sidewall implant. From the point of view of the off-state leakage current, the sample with the sidewall implant is totally hardened to 100 krad(Si), while for the sample without the sidewall implant, the radiation-induced degradation is obvious and the off-state leakage current is approximately 5 orders of magnitude larger than the corresponding pre-irradiation value at 100 krad(Si).

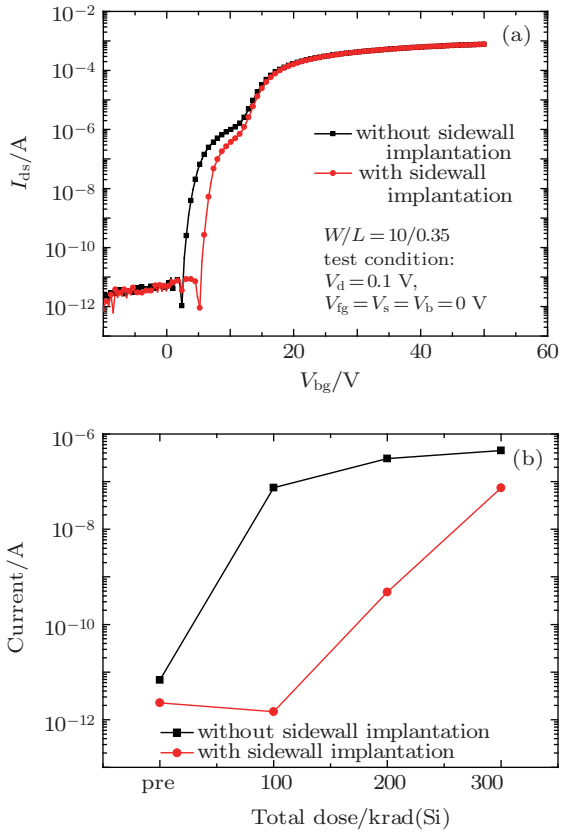


Fig. 9. (color online) (a) Back-gate transfer characteristics and (b) off-state leakage current as a function of total ionizing dose for 10/0.35 PDSOI n-MOSFET with drain biased at 0.1 V. The data of two samples are measured: one sample has the sidewall implant and the other one has not.

4. Conclusion

In summary, the total ionizing dose effects of the 130 nm PDSOI I/O n-MOSFET are discussed in detail. The radiation-induced trapped charge in the STI oxide, but not in the buried oxide, is found to be the main contributor to the intra device off-state leakage after the ON bias radiation. Since the threshold voltage of the STI parasitic transistor is larger than that of the back-gate main transistor, an obvious back-gate hump effect is observed. The threshold voltage of the STI parasitic transistor is a key factor affecting the hardness level of the PDSOI I/O n-MOSFET. A radiation enhanced DIBL effect is observed. The high drain bias will reduce the threshold voltage of the STI parasitic transistor and increase the radiation-induced off-state leakage. Both the high dose well doping and an additional STI sidewall implantation can increase the threshold voltage of the STI parasitic transistor. The increase of the threshold voltage is helpful to improve the total ionizing dose radiation response. The STI sidewall implantation only increases the threshold voltage of the STI parasitic transistor, so it can also suppress the hump effect at the back gate, whereas, the increasing doping concentration in the whole body region raises the threshold voltages of the STI parasitic transistor and the back-gate main transistor simultaneously. It has no benefit for undermining the back-gate hump. As an added bonus, the high body doping will inhibit the radiation-induced coupling effect and reduce the threshold voltage shift in the front gate.

Acknowledgment

The authors are indebted to the Xinjiang Technical Institute of Physics and Chemistry, Chinese Academmy of Science for the radiation experiment and useful discussions.

References

[1] Schwank J R, Shaneyfelt M R and Dodd P E 2013 *IEEE Trans. Nucl. Sci.* **60** 2074
[2] Barth J L, Dyer C S and Stassinopoulos E G 2003 *IEEE Trans. Nucl. Sci.* **50** 466
[3] Fleetwood D M 2013 *IEEE Trans. Nucl. Sci.* **60** 1706
[4] Schwank J R, Shaneyfelt M R, Fleetwood D M, Felix J A, Dodd P E, Paillet P and Ferlet-Cavrois V 2008 *IEEE Trans. Nucl. Sci.* **55** 1833
[5] Oldham T R and McLean F B 2003 *IEEE Trans. Nucl. Sci.* **50** 483
[6] Lukyanchikova N B, Petrichuk M V, Garbar N, Mercha A, Simoen E and Claeys C 2003 *J. Appl. Phys.* **94** 4461
[7] Leray J L, Dupontnivet E, Musseau O, Coic Y M, Umbert A, Lalande P, Pere J F, Aubertonherve A J, Bruel M, Jaussaud C, Margail J, Giffard B, Truche R and Martin F 1988 *IEEE Trans. Nucl. Sci.* **35** 1355
[8] Schwank J R, Ferlet-Cavrois V, Shaneyfelt M R, Paillet P and Dodd P E 2003 *IEEE Trans. Nucl. Sci.* **50** 522
[9] Schwank J R, Shaneyfelt M R, Dodd P E, Burns J A, Keast C L and Wyatt P W 2000 *IEEE Trans. Nucl. Sci.* **47** 604
[10] McLain M, Bamaby H J, Holbert K E, Schrimpf R D, Shah H, Amort A, Baze M and Wert J 2007 *IEEE Trans. Nucl. Sci.* **54** 2210
[11] Dodd P E, Shaneyfelt M R, Schwank J R and Felix J A 2010 *IEEE Trans. Nucl. Sci.* **57** 1747
[12] Liu Z L, Hu Z Y, Zhang Z X, Shao H, Chen M, Bi D W, Ning B X and Zou S C 2011 *Chin. Phys. B* **20** 120703
[13] Liu Z L, Hu Z Y, Zhang Z X, Shao H, Chen M, Bi D W, Ning B X and Zou S C 2011 *Chin. Phys. B* **20** 070701
[14] Hu Z Y, Liu Z L, Shao H, Zhang Z X, Ning B X, Chen M, Bi D W and Zou S C 2011 *Chin. Phys. B* **20** 120702
[15] Shaneyfelt M R, Dodd P E, Draper B L and Flores R S 1998 *IEEE Trans. Nucl. Sci.* **45** 2584
[16] Muller R S and Kamins T I 1986 *Device Electronics for Integrated Circuits* (New York: John Wiley & Sons)
[17] Youk G U, Khare P S, Schrimpf R D, Massengill L W and Galloway K F 1999 *IEEE Trans. Nucl. Sci.* **46** 1830
[18] Cheng Y and Hu C *MOSFET Modeling & BSIM3 User's Guide* (New York: Kluwer Academic Publishers) p. 44
[19] Zhu M, Lin Q, Zhang Z X and Lin C L 2003 *Chin. Phys. Lett.* **20** 767
[20] Ferlet-Cavrois V, Gasiot G, Marcandella C, D'Hose C, Flament O, Faynot O, de Pontcharra J D and Raynaud C 2002 *IEEE Trans. Nucl. Sci.* **49** 2948
[21] Celler G K and Cristoloveanu S 2003 *J. Appl. Phys.* **93** 4955
[22] Wolf S and Tauber R N *Silicon Processing for the VLSI Era* (Vol. 4) (California: Lattice Press) p. 435